NEUTRON CROSS-SECTIONS AND REACTION PRODUCTS FOR H, C, N, AND O FOR THE ENERGY RANGE FROM THERMAL TO 15 MEV*

J. A. AUXIER and M. D. BROWN

Health Physics Division, Oak Ridge National Laboratory, Oak Ridge, Tennessee

Abstract—The accurate calculation of neutron dose must be based on definitive cross-sections and a precise knowledge of the reaction products in tissue. Although there are still several uncertainties in these parameters, a compilation has been made of the most detailed cross-section data available and reaction products for the four major elements in tissue (i.e. H, C, N, and O). The compilation is for neutron energies below 15 MeV, but the energy interval requiring the most study and analysis was that from 2.5 to 15 MeV. Particular attention was directed to the non-elastic reactions [e.g. the $C(n,n^1)3\alpha$ reaction]. Average values for the energies of the various charged particles as a function of the energy of the incident neutron have been computed. These values were compiled to provide a basis for revision of the dose-distribution functions for neutron exposures of man and of animals used in radiobiological studies. An analysis of the results of various measurements are compared with calculated values based on these cross-sections and with the values listed in NBS Handbook 63.

ANY absolute measurement of neutron fluence or any calculation of "dose" from fluence requires a knowledge of neutron cross-sections for the materials of interest. For some applications, only an activation cross section is required, and in some instances only elastic cross-sections are needed. However, the health physicist must have available the best cross-sections for many types of reactions because his interests and activities are so broad. Of particular interest are the cross-sections of the principal elements in tissue: hydrogen, carbon, nitrogen, and oxygen, for neutrons. The values for the thermal neutron cross-sections for these materials have not changed greatly during the past ten years, and those for the region below 2.5 MeV have changed in a few instances only. For higher energies the changes have been greater, for the neutron energy span from about 6 to 14 MeV, many uncertainties have been encountered and many changes made in recent years and until the present. This has resulted in frequent changes in accepted values at most laboratories. Similarly, there have been considerable uncertainties in the reaction products, both in terms of particle or quantum types[1] and in values for the energy released by the specific reaction products; Q values[2] have been known generally for about a decade. The formation of nuclear data information centers such as those at Oak Ridge National Laboratory and at Brookhaven National Laboratory has made the compilations easier; in the future, they may provide most of the information in the form needed. However, due to the special nature of the dosimetry requirements, the information presented here was taken from many sources and averages and interpolations made as required for a computation of absorbed dose in the energy range below 15 MeV. For neutron energies of 2.5 to 15 MeV, a smooth curve based on extrapolation between the available data points is generally a good approximation of the cross-section curves for dosimetry applications. Figure 1 shows the elastic scattering cross-section[3] of the four principal elements in tissue for the energy range below 14 MeV. The relative macroscopic cross-section

* Research sponsored by the U.S. Atomic Energy Commission under contract with the Union Carbide Corporation.

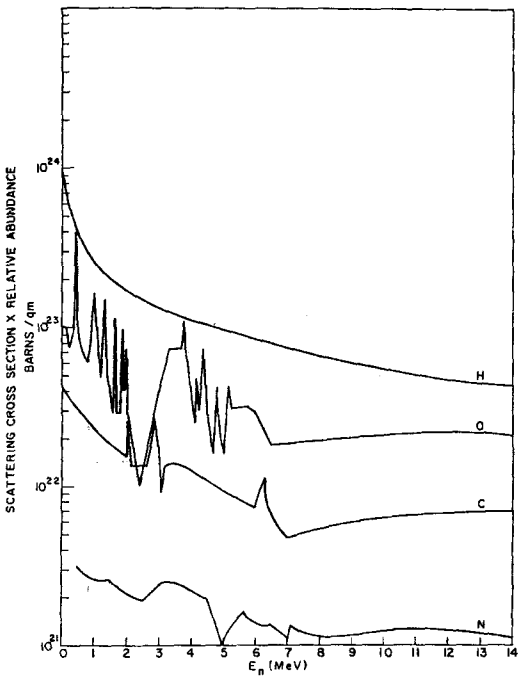

FIG. 1. Macroscopic elastic scattering cross-sections for the H, O, C, and N in tissue for the neutron energy range from thermal to 14 MeV.

has the advantage here that the relative number of interactions with each element can be seen readily. The relative contribution of the C, N, and O recoils to dose equivalent is greater than for absorbed dose because of the higher average values of LET (i.e. greater QF's). The elastic cross-sections are generally decreasing functions of neutron energy to 15 MeV.

Two of the cross-sections for neutrons of thermal and near-thermal energies are shown in Fig. 2.[3] These cross-sections, decreasing with neutron energy as $1/V$, have been accepted generally for some time. The only important reactions are the ${}^{1}_{1}\mathrm{H}(n,\gamma){}^{2}_{1}\mathrm{H}$ and the ${}^{14}_{7}\mathrm{N}(n,p){}^{14}_{6}\mathrm{C}$ reactions [e.g. all other (n,γ) reactions total about 0.5% of the ${}^{1}_{1}\mathrm{H}(n,\gamma){}^{2}_{1}$ reaction].

All significant nonelastic cross-sections for neutrons incident on tissue are shown in Fig. 3.[3] These are relative macroscopic values with all proton-producing reactions, all alpha-producing reactions, etc., summed. These threshold reactions are generally increasing functions

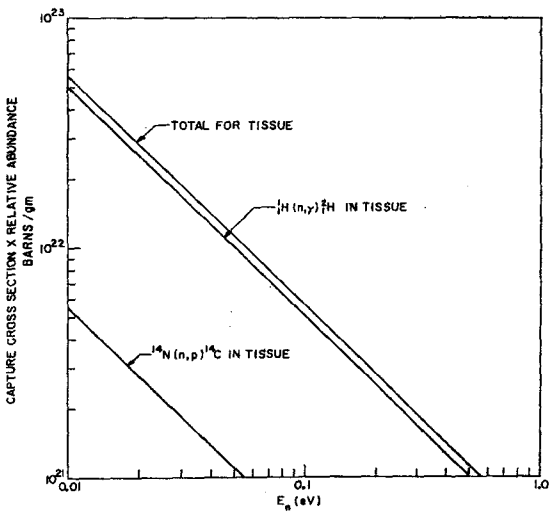

FIG. 2. Macroscopic capture cross-sections for the H and N in tissue for the thermal and near-thermal neutron energy range.

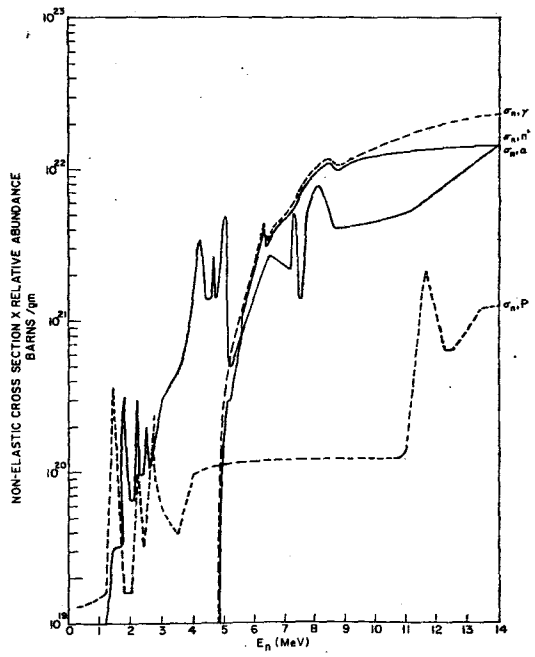

FIG. 3. Total macroscopic nonelastic cross-sections for tissue for the energy range from thermal to 14 MeV.

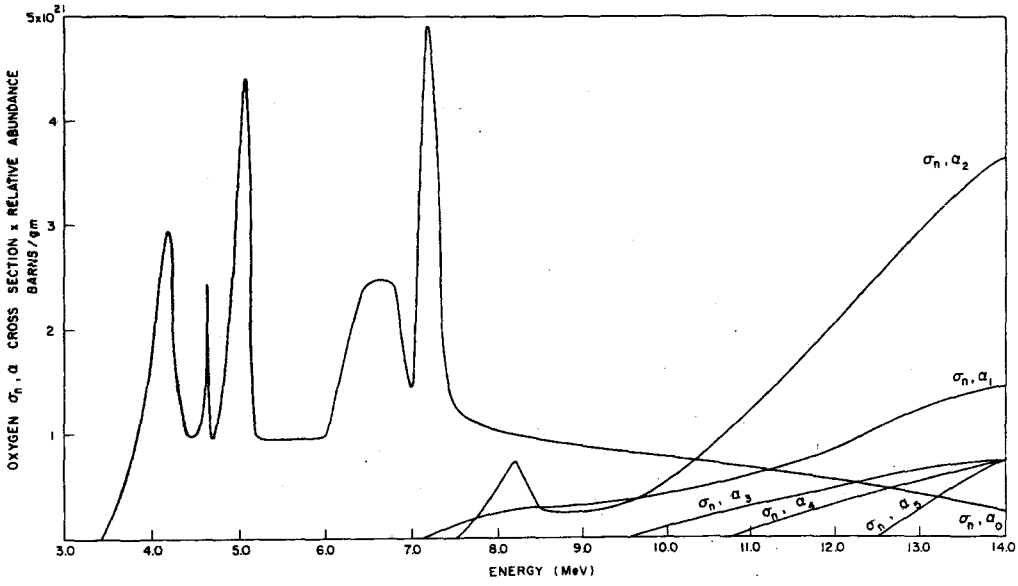

FIG. 4. Total oxygen cross-sections for alpha-producing reactions in tissue for the neutron energy range from 3 MeV (below the lowest threshold) to 14 MeV.

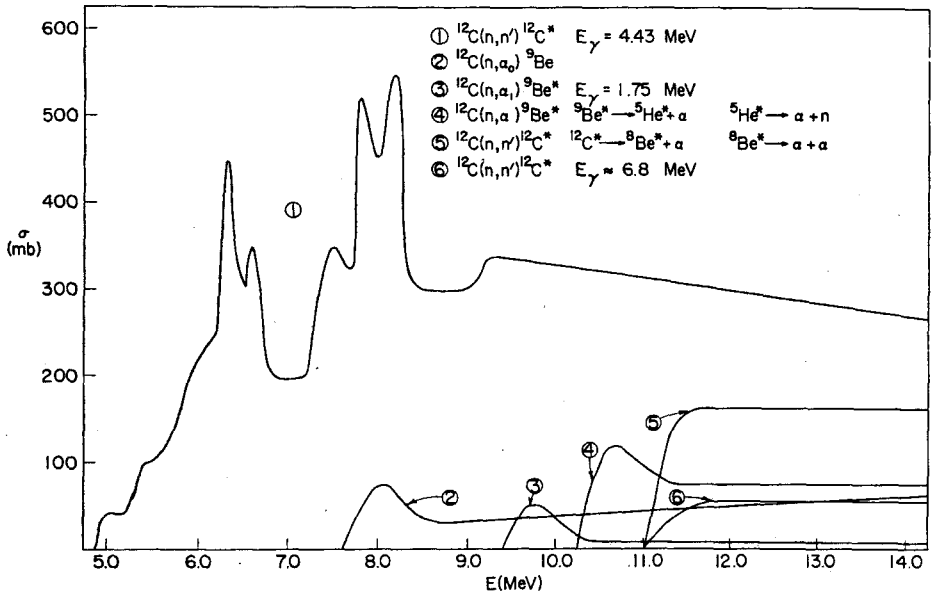

FIG. 5. Microscopic cross-sections for inelastic and nonelastic reactions in ^{12}C for the neutron energy range from 5 MeV to 14 MeV.

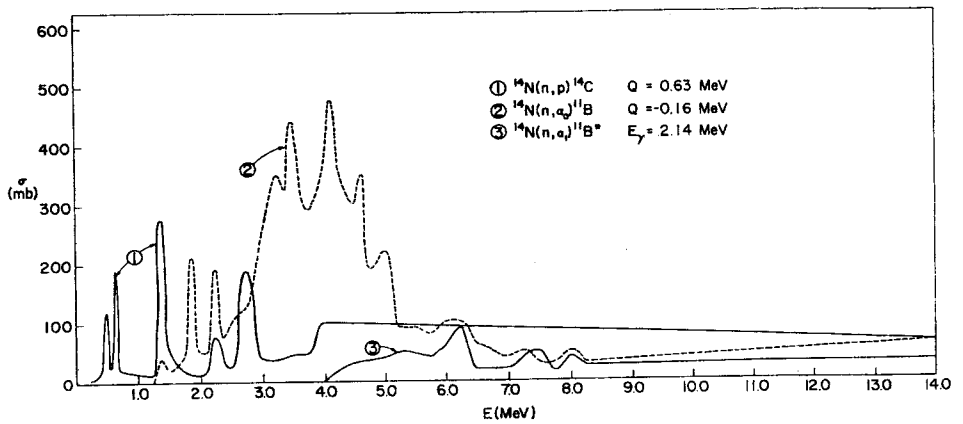

FIG. 6. Microscopic cross-sections for the three reactions, $^{14}N(n,p)^{14}C$, $^{14}N(n,\alpha_0)^{11}B$, and $^{14}N(n,\alpha_1)^{11}B^*$, for the energy range from thermal to 14 MeV.

of energy to 15 MeV. The sum of the macroscopic (n,γ) reaction cross-sections is shown as a separate curve; the sum includes the cross-sections of charged particle reactions which yield de-excitation gamma-rays [e.g. $^{12}C(n,n')^{12}C^*$]. This curve is not the sum of the other curves because some charged particle reactions do not yield gamma-rays [e.g. the $^{12}C(n,n')3\alpha$]. Some of the reactions [e.g. $^{14}N(n,p)^{14}C$] yield greater energy for local deposition than the incident neutron (i.e. they have positive values of Q).

Cross-sections for reactions which cause alpha-particle emission from oxygen nuclei are shown in Fig. 4.[3-13] Although these general values are convenient for estimating dose or

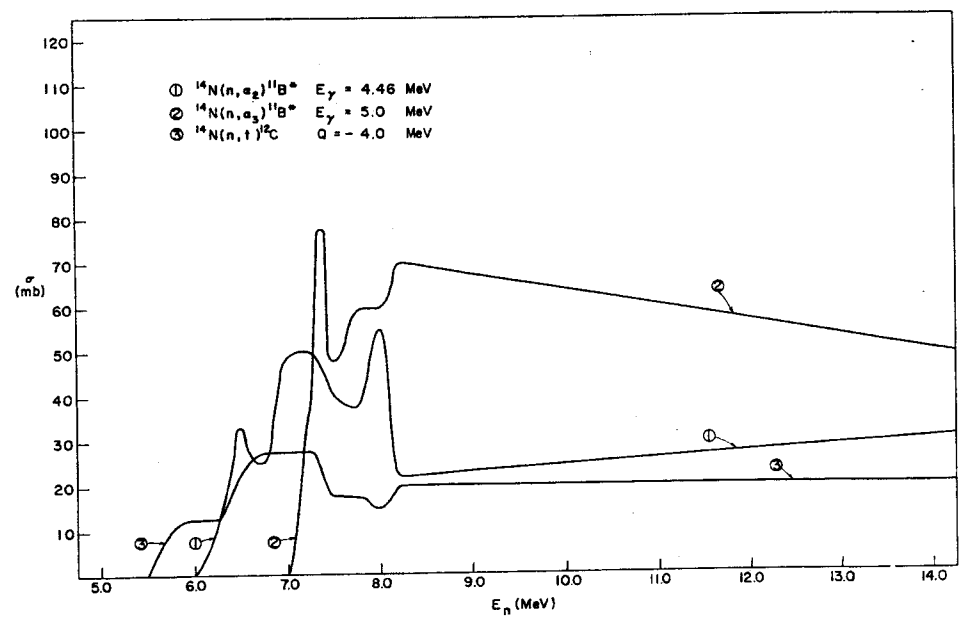

FIG. 7. Microscopic nonelastic cross-sections for the three reactions, $^{14}N(n,\alpha_2)^{11}B^*$, $^{14}N(n,\alpha_3)^{11}B^*$, and $^{14}N(n,t)^{12}C$, for the neutron energy range from 5 MeV to 14 MeV.

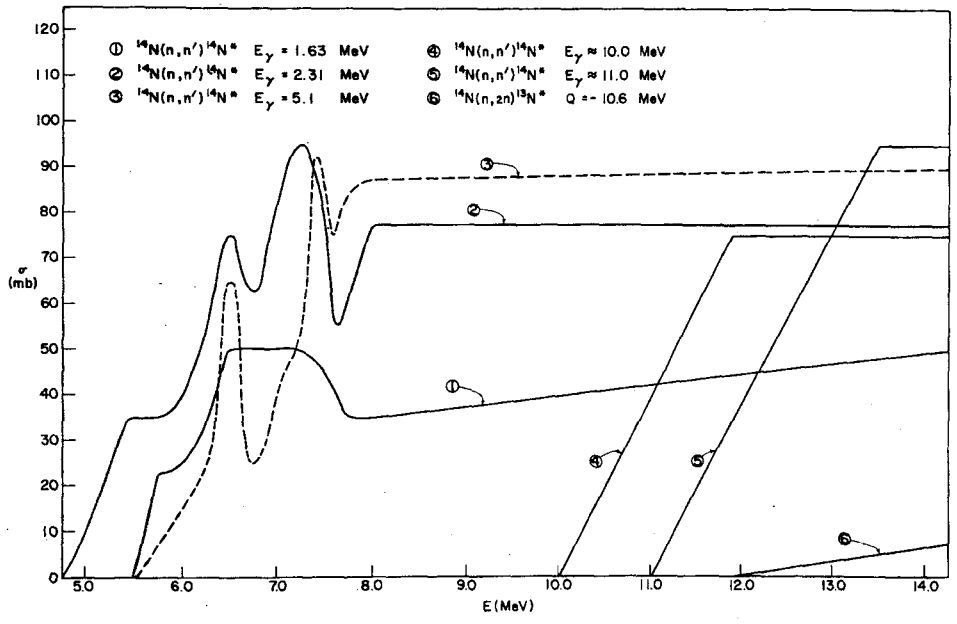

FIG. 8. Microscopic inelastic cross-sections for five (n,n') and one $(n,2n)$ reactions in ^{14}N for the energy range from 4.75 MeV to 14 MeV.

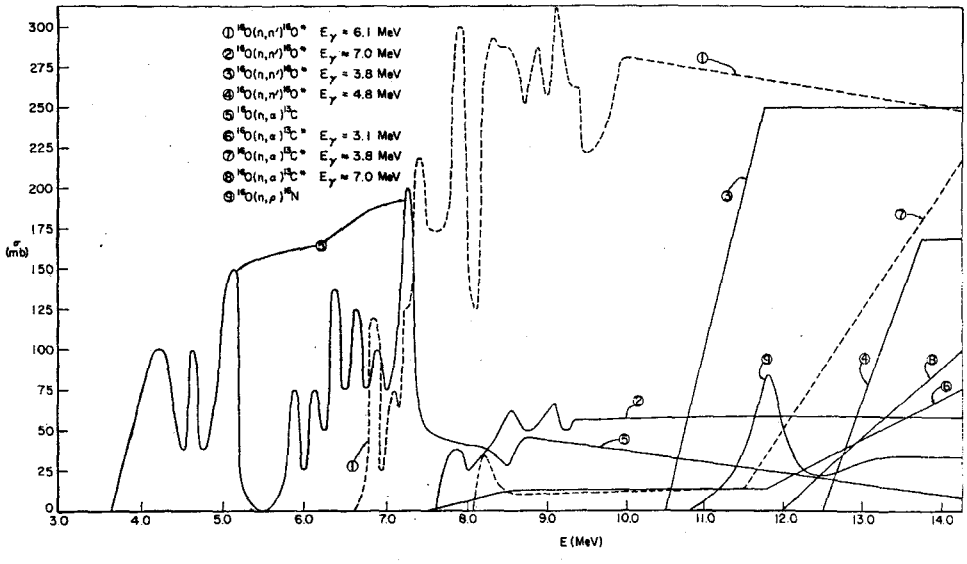

FIG. 9. Microscopic inelastic and nonelastic cross-sections for ^{16}O for the neutron energy range from 3 MeV to 14 MeV.

Reaction	Q Value (MeV)	E_n = 14 MeV		EI = 7 MeV	
		E_{max} (MeV)	R_{max} (cm)	E_{max} (MeV)	R_{max} (cm)
$^{12}C(n, \alpha)^{9}Be$	−5.70	7.89	6.5×10^{-3}	1.28	3.8×10^{24}
$^{14}N(n, p)^{14}C$	0.63	14.6	2.23×10^{-1}	7.62	6.90×10^{-2}
$^{14}N(n, t)^{12}C$	−4.01	9.67	4.5×10^{-2}	2.98	6.3×10^{-3}
$^{14}N(n, \alpha)^{11}B$	−0.16	12.8	1.5×10^{-2}	6.30	4.5×10^{-3}
$^{16}O(n, p)^{16}N$	−9.63	4.19	2.38×10^{-2}	0	0
$^{16}O(n, d)^{15}N$	−9.90	4.03	1.34×10^{-2}	0	0
$^{16}O(n, \alpha)^{13}C$	−2.21	11.04	1.17×10^{-2}	4.57	2.6×10^{-3}

FIG. 10. Charged particle reactions in tissue with maximum ranges for 14 MeV and 7 MeV neutrons.

dose equivalent, an extensive set of cross-sections are required for detailed calculations; the detailed non-elastic and inelastic cross sections are given in Figs. 5 through 9.[3-13] Figure 10 shows a list of the most important charged particle reactions by neutrons in tissue. The maximum ranges for the charged particles for 7 and 14 MeV neutrons are shown as are the accepted Q values. The equation used to compute the average energy deposited by a charged particle is given below. This equation is based on an assumed particle emission with equally probable energies between zero and maximum.

$$E_2 = \frac{2 M_1 M_2 E_1}{(M_2 + M_3)^2} + \frac{M_3 Q + E_1 (M_3 - M_1)}{M_2 + M_3}$$

where: M_1 = mass of incident particle,
M_2 = mass of reaction product with energy E_2,
M_3 = mass of reaction product with energy $E_3 = E_1 + Q - E_2$,
Q = Q value of reaction,
E_1 = energy of incident particle, and
E_2 = average energy of reaction product with mass M_2.

A more comprehensive presentation and analysis of the calculational results will be presented in a paper by Jones *et al.*[14]

REFERENCES

1. F. AJZENBERG-SELOVE and T. LAURITSEN. *Nucl. Phys.* **11,** 1 (1959).
2. F. EVERLING *et al. 1960 Nuclear Data Tables,* Parts 1 and 2, Nuclear Data Project, NAS-NRC (Edited by K. Way) (1961).
3. D. J. HUGHES and R. B. SCHWARTZ. *Neutron Cross-Sections.* Brookhaven National Laboratory Report BNL-325, 2nd edition (1958).
4. D. J. HUGHES, B. A. MAGURNO, and M. K. BRUSSEL. *Neutron Cross Sections.* Brookhaven National Laboratory Report BNL-325, 2nd edition, Supplement 1 (1960).
5. J. R. STEHN *et al. Neutron Cross Sections.* Brookhaven National Laboratory Report BNL-325, 2nd edition, Supplement 2, volume 1 (1964).
6. J. R. SMITH. *Phys. Rev.* **95,** 730 (1954).
7. A. B. LILLIE. *Phys. Rev.* **87,** 716 (1952).
8. W. J. MCDONALD *et al. Nucl. Phys.* **75,** 353 (1966).
9. V. V. NEFEDOV *et al. Soviet Progress in Neutron Physics* (Edited by P. A. KRUPCHITSKII), pp. 241–247 (1961).
10. R. A. AL-KITAL and R. A. PECK, JR. *Phys. Rev.* **130,** 1500 (1963).
11. V. E. SCHERRER, R. B. THEUS, and W. R. FAUST. *Phys. Rev.* **91,** 1476 (1953).
12. J. P. CONNER. *Phys. Rev.* **89,** 712 (1953).
13. J. B. SINGLETARY and D. E. WOOD. *Phys. Rev.* **114,** 1595 (1959).
14. T. D. JONES *et al.* Dose distribution functions for neutrons and gamma rays in anthropomorphous and radiobiological phantoms (see first article of Session 24 of these Proceedings).

DISCUSSION

G. JOYET (*Switzerland*):

Ich möchte fragen ob Sie mit den gleichen Koeffizienten die Gonadendosis für den Mann und für die Frau bestimmen können und wo Sie ihr Dosimeter anbringen.

E. PIESCH (*Germany*):

Das beschriebene Phosphatglasdosimeter II zeigt an der Phantom-Oberfläche einen in gleicher Weise zur Energiedosis in den Gonaden (Hoden) und zur Energiedosis im Knochenmark proportionalen Messwert an. Nach Messungen von Jones erhält man für die weiblichen Gonaden (Eierstöcke) dieselbe Energieabhängigkeit der Energiedosis wie für das Knochenmark. Der Messwert des Personendosimeters entspricht daher den Energiedosen in den männlichen und weiblichen Gonaden sowie der Energiedosis im Knochenmark. Die Phantombestrahlungen wurden im Strahlungsfeld einer hartgefilterten Röntgenbremsstrahlung durchgeführt. Das Personendosimeter wurde hierbei auf der Phantomvorderseite in Brusthöhe aufgehängt. Die Messwerte beziehen sich nur auf eine frontale Strahleneinfallsrichtung.

D. NACHTIGALL (*Euratom*):

Können Sie noch einige Angaben zum transportablen Gerät machen: wie ist das Gewicht, der Gasdruck und die Richtungsabhängigkeit? Welche mittleren QF sind in der Umgebung von Hochenergiebeschleunigern gemessen worden?

H. ŻARNOWIECKI (*Poland*):

1. Bis heute ist nur ein Prototyp konstruiert. Das Gewicht des Gerätes wird 3–4 kg sein. Der Gasdruck hängt von dem Modell ab. Der mittlere Gasdruck ist 6 Atü. Die Richtungsabhängigkeit ist Funktion des Modells. Es kann nach Wunsch fast isotropisch sein. Mehrere Messungen sind am Phantom gemacht worden.

2. Die QF wurden in der Umgebung von Hochenergiebeschleunigern gemessen und sind publiziert. Ich kann Ihnen die Literatur dazu angeben.

D. BLANC (*France*):

Je voudrais faire un commentaire. Les chambres d'ionisation à remplissage de diélectriques liquides constituent, à mon avis, d'excellents détecteurs à recombinaison. Les points de concours des paliers s'alignent, sur l'axe des abscisses, dans l'ordre des transferts linéaires d'énergie, qu'il s'agisse de rayonnements purs ou mixtes. Nous avons réalisé, en liaison avec le Commissariat à l'Énergie Atomique, des détecteurs cylindriques, parfaitement stables en fonction du temps, dont nous avons d'ailleurs parlé lors de notre communication à ce Congrès. Je pense qu'il y a là une voie de recherche très fructueuse.

G. COWPER (*Canada*):

What is the upper limit of dose rate which may be detected without ambiguity of LET and rate effects?

K. ŻARNOWIECKI:

The upper limit of dose when volume recombination does not exist depends on QF and ranges from 10 to more than 200 rem/hr.

J. A. AUXIER (*U.S.A.*):

Did you use the threshold detector system complete with boron ball? (*Answer*: Yes.)

Due to the relatively large size of the boron ball compared to the phantom, I would expect the type divergence you observed due to the highly different composition and consequent shift of the effective center of detection.

R. E. SIMPSON:

The center of detection, in this small phantom, of the threshold foils shifts with depth. This is significant when compared with the small center of mass of the ion chamber. Therefore a divergence in depth dose measurement would be expected. The threshold foil system is not the most satisfactory system for depth dose measurements of neutrons.

M. E. WRENN (*U.S.A.*):

Have you looked at the long term retention of Be^7? Workers in the 40's found tenacious retention in bone, which may show a longer half-time than that in the whole body. Have you followed the body burden for a longer period to see if the retention curve might show two compartments?

G. LEGEAY:

Notre étude ne concernant que la formation du Be^7 en vue d'une investigation dosimétrique après accident, nous n'avons envisagé son devenir que pendant un temps relativement court. Une étude du métabolisme du Béryllium *in vivo* après irradiation protonique est envisagée.